Dalton Transactions

PAPER

View Article Online
View Journal

Cite this: DOI: 10.1039/c5dt02264a

Tricarbonyl ^{99m}Tc(I) and Re(I)–thiosemicarbazone complexes: synthesis, characterization and biological evaluation for targeting bacterial infection†

Dipak Kumar Nayak,[a] Rinku Baishya,[a] Ramalingam Natarajan,[b] Tuhinadri Sen[c] and Mita Chatterjee Debnath*[a]

Received 15th June 2015,
Accepted 4th August 2015

DOI: 10.1039/c5dt02264a

www.rsc.org/dalton

Methyl, ethyl and phenyl nitrofuryl thiosemicarbazone ligands (**1**, **2** and **3** respectively) were radiolabeled with freshly prepared aqueous solution of a *fac*[^{99m}Tc(CO)$_3$(H$_2$O)$_3$]$^+$ precursor. The radiochemical yield was around 98% as determined by thin layer chromatography and HPLC. The complexes exhibited substantial stability. The corresponding Re(I) complexes were prepared from a Re(CO)$_5$Br precursor to understand the coordination behavior of the ligands against a tricarbonyl rhenium(I) precursor. The rhenium(I) complexes were characterized by means of IR, NMR and mass spectroscopic studies as well as by X-ray crystallography, and correlated with the technetium complexes by means of HPLC studies. Electrochemical reduction of monomeric Re(CO)$_3$-complexes of nitrofuryl ethyl thiosemicarbazone was also studied using cyclic voltammetry. Biodistribution studies of ^{99m}Tc(CO)$_3$-labeled thiosemicarbazones in rats intramuscularly infected with *S. aureus* exhibited substantial *in vivo* stability of the complex and moderate accumulation at the site of focal infection.

Introduction

Over the last few years the chemistry of thiosemicarbazone complexes of transition metals has been receiving considerable attention largely because of their wide range of biological properties specially as antifungal, antibacterial, antiviral and anticancer agents.[1–4] Thiosemicarbazones with the general formula $R^1R^2C{=}N{-}NH{-}CS{-}NR^3R^4$ usually react as versatile chelating ligands and can coordinate with different transition metal ions [*e.g.* Cu(II), Cr(III), Co(III), Ni(II) *etc*.] by bonding through the sulfur and hydrazinic nitrogen atoms.[5–8] The metal complexes show better biological activities as compared to the free thiosemicarbazones.[9–11] Nitrofuryl thiosemicarbazones (NFT) have also been investigated as antibacterial and antiprotozoal drugs.[12,13] The electrochemical reduction of nitro heterocyclic compounds follows a complex and well known mechanism which is a prerequisite for their antibacterial activity.[14,15] The highly reactive electrophilic intermediate produced by the action of bacterial nitroreductases on NFT is postulated to affect bacterial DNA.[3,16] Some pieces of evidence suggest that the reduced NFT binds to bacterial ribosomes and prevents protein synthesis.[17] NFTs exert greater effects on bacterial cells than on mammalian cells because bacterial cells activate the drug more rapidly.[18,19] Naturally, the preparation of transition metal complexes of thiosemicarbazones containing the nitrofuryl pharmacophore and studies on their antibacterial and antiparasitic activities are the areas receiving much attention.[12,13,20]

Technetium-99m is a transition metal and the most widely used SPECT radionuclide in nuclear medicine that aids in the diagnosis of various medical conditions.[21–23] In the pursuit of novel pharmacophores for use in infection diagnosis by scintigraphic imaging, we have already reported the labeling of nitrofuryl thiosemicarbazones and a wide variety of fluoroquinolones with the *fac*[^{99m}Tc(CO)$_3$(H$_2$O)$_3$]$^+$ precursor.[24] Considering the importance of nitrofuryl thiosemicarbazones, we prepared ^{99m}Tc(CO)$_3$ chelates of methyl, ethyl and phenyl nitrofuryl thiosemicarbazone ligands (**1**, **2** and **3** respectively)

[a]*Infectious Disease and Immunology Division, Indian Institute of Chemical Biology (CSIR), 4, Raja S. C. Mullick Road, Jadavpur, Kolkata-700032, India. E-mail: mita_chdebnath@yahoo.com, mitacd@iicb.res.in; Fax: +91 33-2473-5197, +91 33-2472-3967; Tel: +033-2473 3491*

[b]*Chemistry Division, Indian Institute of Chemical Biology (CSIR), 4, Raja S. C. Mullick Road, Jadavpur, Kolkata-700032, India*

[c]*Department of Pharmaceutical Technology, Jadavpur University, Kolkata-700032, India*

†Electronic supplementary information (ESI) available: NMR, mass, IR spectra, HPLC-figures, table of selected bond angles and CIF files giving X-ray crystallographic data. CCDC 878521, 1402565, 1017880, 1017882, 1017879 and 1402539 for Re(CO)$_3$-**1**, *trans*-[ReBr(CO)$_3$-**1a**], Re(CO)$_3$-**2**, *trans*-[ReBr(CO)$_3$-**2a**], *cis*-[ReBr(CO)$_3$-**2b**] and Re(CO)$_3$-**3**. For ESI and crystallographic data in CIF or other electronic format see DOI: 10.1039/c5dt02264a

of varying lipophilicities and investigated the influence of the physicochemical behavior of the complexes on biological activities in the present study.

As a part of our efforts, we also tried to understand the coordination behavior of nitrofuryl thiosemicarbazones against the tricarbonyl rhenium(I) precursor. A series of thiosemicarbazone complexes were therefore prepared from $Re(CO)_5Br$, which proved to be an excellent starting material for the synthesis of tricarbonyl rhenium(I) complexes. Thiosemicarbazones are versatile ligands that can coordinate either as neutral ligands or in their deprotonated form. Both monomeric $[ReBr(CO)_3\text{-}LH]$ and dimeric $\{[Re(CO)_3\text{-}L]_2\}$ complexes were produced and characterized by X-ray crystallographic and spectroscopic studies. Electrochemical studies were carried out in order to determine the reduction potential of the nitroaromatic group. Thiosemicarbazones act in both types of complexes as bidentate N, S donors. $^{99m}Tc(CO)_3$ labeled thiosemicarbazones exhibited excellent stability in *in vitro* and *in vivo* systems. Initial evaluations of the $^{99m}Tc(CO)_3$-complexes in the *S. aureus* infected rat model were also performed.

Results and discussion

Synthesis and spectroscopic characterization

Thiosemicarbazones **1–3** were synthesized in good yields (75–78%) by mixing equimolar amounts of nitrofurfural and thiosemicarbazide derivatives in toluene (Scheme 1). A red colored amorphous powder was precipitated from the reaction mixtures and was recrystallised from ethanol–water. The mother liquor was concentrated to recover more products. IR, NMR, mass spectroscopy and elemental analysis studies were conducted to characterize the synthesized thiosemicarbazone derivatives.

The pure thiosemicarbazone derivatives thus obtained were reacted with $Re(CO)_5Br$ in toluene to produce $Re(CO)_3$–thiosemicarbazone complexes (Scheme 1) in good yields (74–78%). HPLC analysis of the reaction mixture showed one sharp peak [RT = 13.9 min for $\{Re(CO)_3\text{-}\mathbf{1}\}$, 14.2 min for $\{Re(CO)_3\text{-}\mathbf{2}\}$, and 16.1 min for $\{Re(CO)_3\text{-}\mathbf{3}\}$], attributed to the formation of monomeric rhenium(I) complexes. Slow evaporation of the reaction mixture from $Re(CO)_3$-**2** furnished two different crystals of monomers with different HPLC elution profiles [HPLC peaks

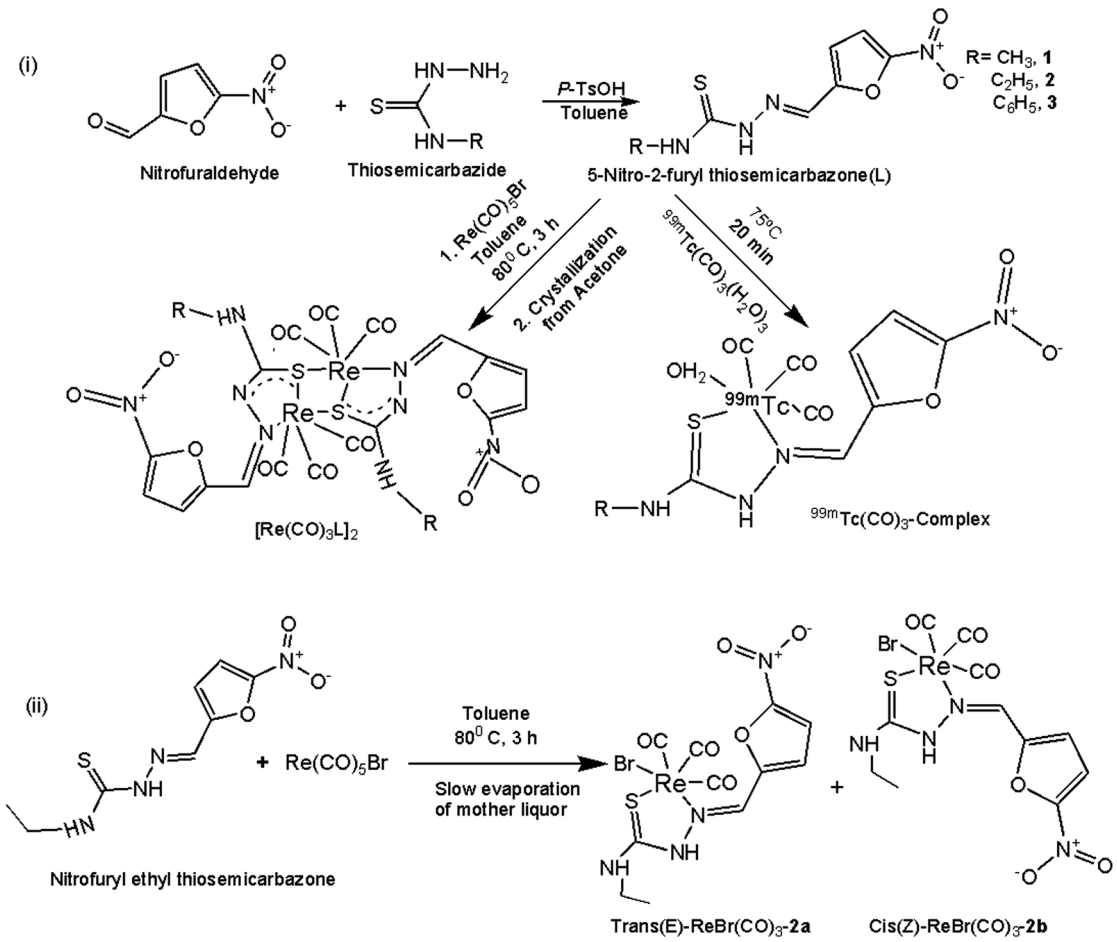

Scheme 1 Synthesis of ligands and complexes.

Table 1 HPLC retention times for ^{99m}technetium(I) and rhenium(I) complexes

Compound	Retention time (min)
^{99m}Tc(I)-synthon	5.1
^{99m}Tc(CO)$_3$-**1**	14.0
^{99m}Tc(CO)$_3$-**2**	14.2
^{99m}Tc(CO)$_3$-**3**	16.1
Re(CO)$_3$-**1** (monomeric)	13.9
[Re(CO)$_3$-**1**]$_2$	15.8
Re(CO)$_3$-**2** (monomeric)	14.2
trans-[ReBr(CO)$_3$-**2a**]	14.2
cis-[ReBr(CO)$_3$-**2b**]	15.8
[Re(CO)$_3$-**2**]$_2$	16.3
Re(CO)$_3$-**3** (monomeric)	16.1
[Re(CO)$_3$-**3**]$_2$	17.3

at 14.2 min for *trans*-ReBr(CO)$_3$-**2a** and 15.8 min for *cis*-ReBr(CO)$_3$-**2b**]. The HPLC retention times thus suggest that the *trans*-monomer was initially formed, which got isomerised during slow evaporation to produce the mixture of isomers. Only one monomer (*trans*) could be isolated from the reaction mixture for ReBr(CO)$_3$-**1** though evidence for the formation of another, uncharacterized product could be obtained. On the other hand, the concentration of the reaction mixtures led to precipitates which could be crystallized. A HPLC study of the products showed another sharp peak at later time points than those mentioned above, attributed to the formation of dimeric rhenium(I) complexes (Table 1).

The mass spectra of the monomeric complexes contain signals corresponding to the molecular ion, although $[M - Br]^+$ formed the base peak. However with dimeric Re(CO)$_3$–thiosemicarbazone complexes, the $[M/2 + H]^+$ species resulting from the symmetric cleavage of the dimeric molecule formed the base peak. A facial geometry around the rhenium atom in all the complexes was suggested by two or three strong IR bands (sometimes collapsed) for ν(CO) bond stretching in the range 1909–2029 cm^{-1}. The N–H group stretching bands appeared at 3252–3400 cm^{-1}. In the NMR spectrum, the proton signals of furan hydrogen appeared deshielded (by around 0.5 ppm) with respect to the free ligand. Other proton signals remained nearly unchanged after co-ordination.

Crystallographic studies of Re(CO)$_3$-complexes

As described above, the precipitate obtained by concentrating the reaction mixture from the Re(CO)$_3$-complex of ligand **1** was dissolved in acetone containing few drops of ethanol, when single crystals containing one molecule of acetone, [Re(CO)$_3$-**1**]$_2$·C$_3$H$_6$O were formed. The complex was dimeric in nature, and the molecular structure is shown in Fig. 1. The ligand coordinates with the metal centre through the sulfur and azomethine nitrogen atoms. The rhenium atom is octahedrally coordinated and interacts with two sulfur atoms, and the two Re–S distances differ by about 0.1 Å, the values of Re1–S2 (S from neighboring monomer) and Re1–S1 (S from the same monomer) being 2.559 and 2.444 Å respectively. These are in accordance with the reported values of rhenium tricarbonyl

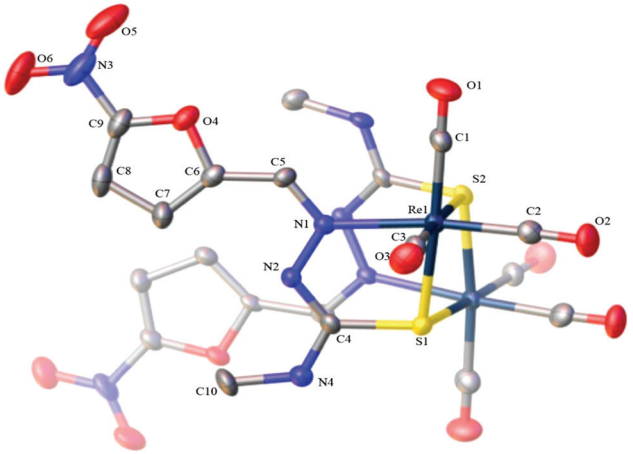

Fig. 1 Molecular structure of [Re(CO)$_3$-**1**]$_2$ with the atom-numbering scheme, showing 30% probability displacement ellipsoids. Solvent molecules have been omitted for the sake of clarity. Selected bond lengths (Å): Re1–C1 1.928(7), Re1–C2 1.912(7), Re1–C3 1.894(7), C1–O1 1.136(7), C2–O2 1.146(7), C3–O3 1.147(7), Re1–N1 2.174(5), Re1–S1 2.4446(16), Re1–S2 2.5596(16), and S1–C4 1.763(5).

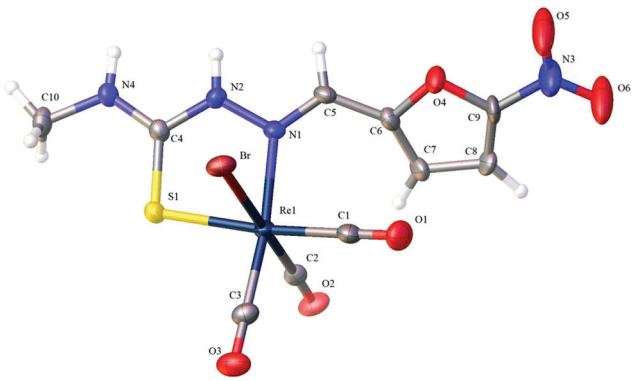

Fig. 2 Molecular structure of *trans*-(*E*)-ReBr(CO)$_3$-**1a** with the atom-numbering scheme, showing 30% probability displacement ellipsoids. Solvent molecules have been omitted for the sake of clarity. Selected bond lengths (Å): Re1–C1 1.891(7), Re1–C2 1.937(7), Re1–C3 1.934(7), C1–O1 1.156(13), C2–O2 1.146(8), C3–O3 1.163(8), Re1–N1 2.226(5), Re1–S1 2.4679(17), S1–C4 1.700(6), Re1–Br1 2.6688(8).

complexes of other thiosemicarbazone ligands.[25,26] The deprotonation of the ligand causes the replacement of the halogen atom in the coordination sphere of the metal by the sulfur atom of the neighboring monomer.

On the other hand, slow evaporation of the reaction mixture (toluene) of the Re(CO)$_3$ complex of ligand **1** furnished crystals containing one molecule of toluene. X-ray crystallographic analysis revealed (Fig. 2) the formation of a monomeric complex, *trans*-[ReBr(CO)$_3$-**1a**]. The dihedral angle between C6–C5–N1–N2 is −170.5°. In this complex, the metal forms a five membered chelate ring with the azomethine nitrogen and the sulfur atom of the thiosemicarbazone ligand.

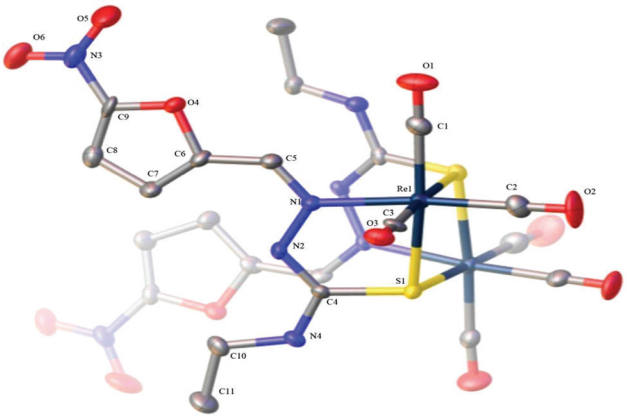

Fig. 3 Molecular structure of $[Re(CO)_3$-**2**$]_2$ with the atom-numbering scheme, showing 30% probability displacement ellipsoids. Solvent molecules have been omitted for the sake of clarity. Selected bond lengths (Å): Re1A–C1A 1.929(13), Re1A–C2A 1.917(15), Re1A–C3A 1.905(16), C1A–O1A 1.127(15), C2A–O2A 1.129(17), C3A–O3A 1.163(18), Re1A–N1A 2.187(9), Re1A–S1A 2.458(3), Re1A–S2A 2.552(3), and S1A–C4A 1.759(13).

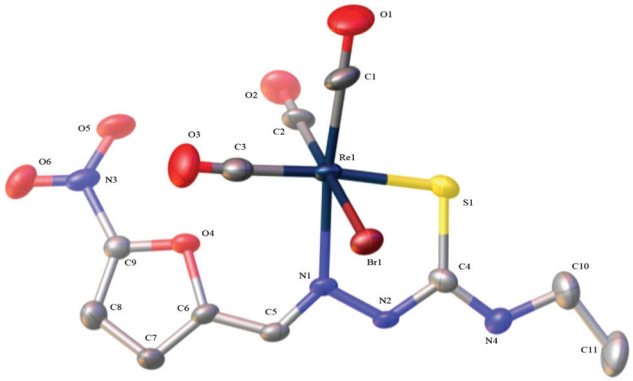

Fig. 4 Molecular structure of *trans*-(*E*)-$ReBr(CO)_3$-**2a** with the atom-numbering scheme, showing 30% probability displacement ellipsoids. Solvent molecules have been omitted for the sake of clarity. Selected bond lengths (Å): Re1–C1 1.892(11), Re1–C2 1.877(10), Re1–C3 1.930(13), C1–O1 1.156(13), C2–O2 1.147(11), C3–O3 1.138(12), Re1–N1 2.215(6), Re1–S 2.466(3), S–C4 1.690(9), and Re1–Br1 2.6627(10).

Similarly, the concentration of the reaction mixture of the $Re(CO)_3$ complex of ligand **2** resulted in the precipitation of a reddish brown solid that was stable in air, moderately soluble in dichloromethane and highly soluble in acetone. Dark brown single crystals were obtained by slow concentration of solution of the precipitate in acetone and methanol. X-ray diffractometry studies showed it to be the dimeric complex (*cis* isomer), $[Re(CO)_3$-**2**$]_2 \cdot C_3H_6O \cdot CH_3OH$ of ligand **2** (Fig. 3).

Two different types of single crystals were obtained by slow evaporation of the reaction mixture (toluene) of the $Re(CO)_3$ complex of ligand **2**. Each molecule of the complex contains one solvent molecule. The crystals differ in color, size and unit cell parameters. The rhenium atom is octahedrally coordinated to three carbonyl carbon atoms (in the *fac* arrangement), a bromine atom, the azomethine nitrogen and the sulfur atom of the thiosemicarbazone ligand, with which the metal forms a five membered chelate ring. Structure elucidation revealed the formation of two isomeric complexes *trans*-$[ReBr(CO)_3$-**2a**$]$ and *cis*-$[ReBr(CO)_3$-**2b**$]$. In the thiosemicarbazone backbone, the dihedral angle between C6–C5–N1–N2 is −175.2° in the *trans* isomer (Fig. 4) but 4° in the *cis* isomer. No remarkable change in bond lengths was observed for Re–N and Re–S in the two isomers. Selected bond lengths are shown below the respective figures, which represent the molecular structure of the two isomers (**2a** and **2b**) studied by X-ray diffraction. Both the structures show the three carbonyl ligands occupying one face and have a typical Re–C bond distance (~1.87–1.93 Å) of the facial $Re(CO)_3$ unit.

Finally, the concentration of an aqueous methanolic solution of the initial precipitate of the $Re(CO)_3$-complex of ligand **3** furnished single crystals with one molecule of methanol, $[Re(CO)_3$-**3**$]_2 \cdot CH_3OH$. The complex was dimeric in nature, whose molecular structure is shown in Fig. 5. The ligand coordinates with the metal centre through the sulfur and azomethine nitrogen atoms. As described above for **1** and **2**, the thiosemicarbazone ligands were deprotonated in this case also and the halogen atom in the coordination sphere of the metal was displaced by the sulfur atom of the neighboring ligand. Each Re is attached to two sulfur atoms in the dimers, one from the same monomer and the other belonging to the neighboring monomer. There exist a difference of about 0.1 Å in the two Re–S distances. Re–N distances are comparable to the Re–N distances of the other two dimeric complexes. In the case of dimeric and monomeric complexes, no remarkable difference in the Re–N distance was observed.

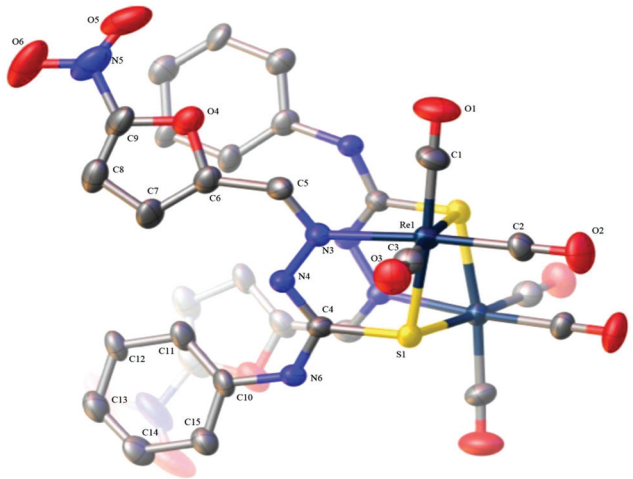

Fig. 5 Molecular structure of $[Re(CO)_3$-**3**$]_2$ with the atom-numbering scheme, showing 30% probability displacement ellipsoids. Solvent molecules have been omitted for the sake of clarity. Selected bond lengths (Å): Re1–C1 1.925(8), Re1–C2 1.916(10), Re1–C3 1.919(8), C1–O1 1.156(11), C2–O2 1.156(11), C3–O3 1.144(10), Re1–N3 2.182(7), Re1–S1 2.4594(19), Re1–$S1^1$ 2.570(2), and S1–C4 1.778(7).

Electrochemical studies

Fig. 6 shows typical voltammograms for monomeric $Re(CO)_3$-complexes of nitrofuryl ethyl thiosemicarbazone. Table 4 lists the values of the first and second cathodic peaks. Voltammetric data indicated one electron reversible transfer (peak IIIc/IIIa) around −0.80 V corresponding to the nitro-anion radical generation while the more negative second peak could be attributed to the production of the hydroxylamine derivative (peak IVc).[27] This study thus reveals the formation of the nitro anion radical as well as the hydroxylamine moiety. All of the metal complexes exhibited lower $E_{1/2}$ ($E_{1/2} = (E_a + E_c)/2$) values than Nifurtimox (−0.88 V) as the reference showing a higher capacity to be reduced, and hence a better ability to generate the radical species.

Voltammograms of all the metal complexes show one anodic peak (Ia) that could be attributed to the reoxidation process of the hydroxylamine RNHOH generated in IVc into RNO. A second sweep exhibits a shoulder near IIc which could be attributed to the cathodic counterpart from the reversible reaction RNHOH ⇄ RNO + $2e^-$ + $2H^+$. Prepeak IIc appears even before the reduction of the nitro group, which seems to follow another reaction path beside the known electron-transfer mechanism of nitroaromatic compounds in aprotic media.[28] Reduction potentials of monomeric rhenium(I) complexes were comparable to the values reported by other workers in this field.

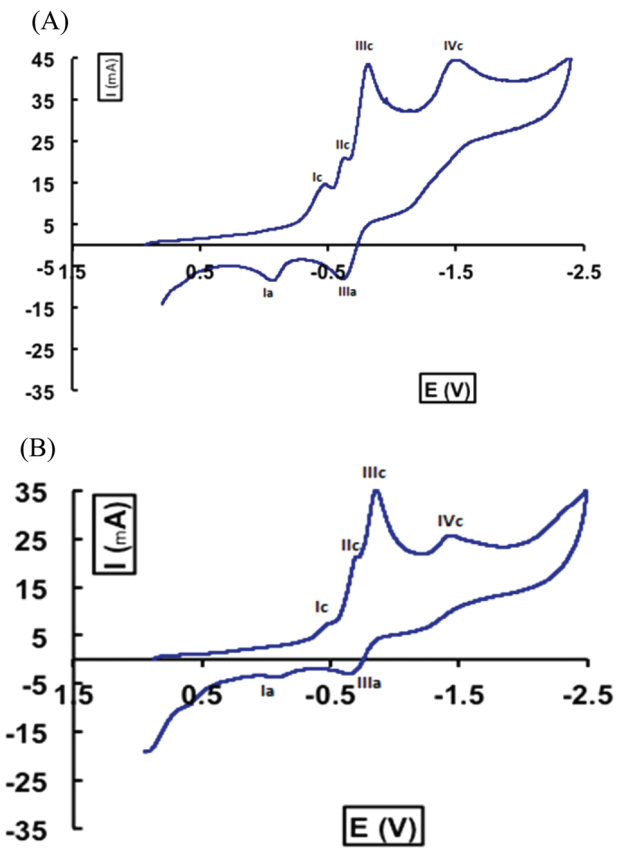

Fig. 6 Cyclic voltammograms at 100 mV s^{-1} of 10 mM solutions of (A) *trans*-[$ReBr(CO)_3$-**2a**] and (B) *cis*-[$ReBr(CO)_3$-**2b**] in DMF containing 0.1 M TBAP.

Radiolabeling and quality control

The ^{99m}Tc(I)-synthon was successfully prepared with more than 98% purity as verified by RP-HPLC (retention time 5.15 min). All three thiosemicarbazone ligands (**1**, **2** and **3**) were successfully labeled with the freshly prepared $[^{99m}Tc(CO)_3(H_2O)_3]^+$ core. Radiolabeling yield depends on the concentration of the ligand, pH of the synthon precursor and ligand solution, and the duration of heating. Complexation was favorable around neutral pH (7.0–7.5). Standardization and optimization studies were performed to obtain maximum complexation. Radiochemical purity of the complexes was routinely checked by thin layer chromatography (ITLC) on silica gel plates and RP-HPLC. For all the complexes, the radiolabeling efficiency was around 98% initially (30 min after preparation). It was around 92% even up to 24 h, indicating the stability of the labeled complexes. Radiochromatograms (Fig. 7) showed a single peak eluting at 14.0, 14.2 and 16.1 min for $^{99m}Tc(CO)_3$-**1**, $^{99m}Tc(CO)_3$-**2** and $^{99m}Tc(CO)_3$-**3** respectively. The chemical identification of ^{99m}Tc-complexes was ascertained by comparison of their HPLC profiles with those of the corresponding rhenium(I) complexes (Table 1). The retention times of ^{99m}Tc-complexes were comparable to those of the corresponding monomeric Re-complexes. It is felt that technetium-99m forms only monomeric complexes due to the high dilution of the tracer.

In vitro stability

The *in vitro* stability of $^{99m}Tc(CO)_3$–thiosemicarbazone complexes in normal saline was checked at various time intervals for up to 24 h. For $^{99m}Tc(CO)_3$-**1**, $^{99m}Tc(CO)_3$-**2** and $^{99m}Tc(CO)_3$-**3** the instant radiolabeling yields were 98.3 ± 0.68%, 97.8 ± 0.84% and 97.7 ± 0.58% respectively. The percentage values of the radiolabeled complex remaining after an incubation of 1 h in saline were 98.2 ± 1.09%, 97.3 ± 1.63% and 97.3 ± 0.97% respectively, which changed to 93.1 ± 2.74%, 91.9 ± 1.74% and 92.0 ± 1.34% after 24 h of incubation.

The *in vitro* serum stabilities of the three $^{99m}Tc(CO)_3$–thiosemicarbazones were monitored by ITLC for up to 24 h at 37 °C. The levels of free radioactive species generated after 24 h of incubation were 8.74 ± 2.51%, 9.64 ± 3.07% and 9.23 ± 2.77% for $^{99m}Tc(CO)_3$-**1**, $^{99m}Tc(CO)_3$-**2** and $^{99m}Tc(CO)_3$-**3** respectively.

Partition coefficient

The logarithm of partition coefficient (log $P_{o/w}$) is a parameter used to provide an indication of the lipophilicity of the complexes. The log $P_{o/w}$ values as determined by partitioning between octanol and phosphate buffer were found to be 0.52 ± 0.06, 0.67 ± 0.07, and 0.86 ± 0.06 for $^{99m}Tc(CO)_3$-**1**, $^{99m}Tc(CO)_3$-**2** and $^{99m}Tc(CO)_3$-**3** respectively indicating the lipophilic nature of the complexes.

Table 2 Crystal data and structure refinement parameters of $Re(CO)_3$–thiosemicarbazone complexes

Compound	*trans*-(*E*)-$ReBr(CO)_3$-**1a**	$[Re(CO)_3$-**1**$]_2$	*trans*-(*E*)-ReBr $(CO)_3$-**2a**	*cis*-(*Z*)-$ReBr(CO)_3$-**2b**	$[Re(CO)_3$-**2**$]_2$	$[Re(CO)_3$-**3**$]_2$
Empirical formula	$C_{13.5}H_{11}N_4O_6ReSBr$	$C_{25}H_{23}N_8O_{14}Re_2S_2$	$C_{18}H_{18}BrN_4O_6ReS$	$C_{18}H_{18}BrN_4O_6ReS$	$C_{52}H_{50}N_{16}O_{28}Re_4S_4$	$C_{32}H_{26}N_8S_2Re_2O_{14}$
Molecular weight	623.43	1096.03	684.53	684.53	2220.12	1183.13
Crystal system	Triclinic	Triclinic	Monoclinic	Monoclinic	Monoclinic	Monoclinic
Space group	$P\bar{1}$	$P\bar{1}$	$P2_1/n$	$P2(1)/c$	$P2_1$	$C2/c$
a (Å)	7.5512(7)	10.154(4)	11.1341(6)	7.0954(6)	9.2120 (8)	24.149(5)
b (Å)	10.6017(9)	10.283(4)	18.3725(10)	13.0042(10)	41.834(4)	12.336(3)
c (Å)	12.8522(12)	18.591(8)	11.6288(6)	25.104(2)	9.7296(9)	13.934(3)
α (°)	94.519(5)	94.160(9)	90	90	90	90°
β (°)	97.975(5)	101.027(9)	101.055(3)	97.113(3)	99.338(4)	111.929(3)
γ (°)	90.201(4)	110.970(8)	90	90	90	90°
V (Å^3)	1015.66(16)	1757.9(12)	2334.7(2)	2298.5(3)	3699.9(6)	3850.7(14)
Z	2	2	4	4	2	4
D_c/g cm^{-3}	2.039	2.071	1.948	1.978	1.993	2.041
μ/mm^{-1}	8.087	7.074	7.046	7.157	6.724	6.467
F(000)	588.0	1046	1312.0	1312.0	2124.0	2272.0
Crystal dimensions (mm)	0.38 × 0.36 × 0.31	0.22 × 0.17 × 0.12	0.23 × 0.21 × 0.19	0.16 × 0.14 × 0.12	0.16 × 0.14 × 0.10	0.22 × 0.2 × 0.2
Theta range for data collection	1.927 to 27.25°	2.15 to 25.00°	2.17 to 25.99	1.63 to 25.00°	1.95 to 27.84	1.81 to 25.99°
Limiting indices	$-9 \le h \le 9$ $-13 \le k \le 13$ $-16 \le l \le 16$	$-12 \le h \le 12$ $-11 \le k \le 12$ $-22 \le l \le 22$	$-13 \le h \le 13$ $-21 \le k \le 22$ $-14 \le l \le 14$	$-7 \le h \le 8$ $-15 \le k \le 15$ $-29 \le l \le 29$	$-11 \le h \le 12$ $-54 \le k \le 54$ $-12 \le l \le 12$	$-29 \le h \le 29$ $-15 \le k \le 13$ $-12 \le l \le 17$
Reflections collected/ unique	18 391/4491 [R(int) = 0.0750]	16 540/6163 [R(int) = 0.0376]	19 069/4570 [R(int) = 0.0594]	16 489/ 3973 [R(int) = 0.0624]	35 570/ 16 427 [R(int) = 0.0392]	9582/3775 [R(int) = 0.0549]
Refinement method	Full-matrix least-squares on F^2	Full-matrix least-squares on F^2	Full-matrix least-squares on F^2	Full-matrix least-squares on F^2	Full-matrix least-squares on F^2	Full-matrix least-squares on F^2
Data/ parameters	4491/260	6163/464	4570/315	3973/ 270	16 427/948	3775/264
Goodness-of-fit on F^2	1.075	1.045	1.037	1.060	1.040	1.018
R indices [$I > 2\sigma(I)$]						
R_1 (on F_o^2, $I > 2\sigma(I)$)	0.0439	0.0284	0.0512	0.0586	0.0378	0.0483
wR_2 (on F_o^2, $I > 2\sigma(I)$)	0.1156	0.0556	0.1181	0.1743	0.0855	0.1378
R indices (all data)						
R_1	0.0509	0.0440	0.0736	0.0737	0.0448	0.0566
wR_2	0.1194	0.0602	0.1318	0.1940	0.0889	0.1528
Largest diff. peaks and holes	1.98 and −1.78e A^{-3}	0.57 and −0.74e A^{-3}	2.35 and −1.61 e Å^{-3}	2.379 and −2.54 e Å^{-3}	1.53 and −1.19e Å^{-3}	3.47 and −1.80e Å^{-3}

In vitro bacterial binding assay

Table 5 represents the results of the bacterial binding assay for $^{99m}Tc(CO)_3$-**1**, $^{99m}Tc(CO)_3$-**2** and $^{99m}Tc(CO)_3$-**3**. Following *S. aureus* incubation, $^{99m}Tc(CO)_3$-**1** exhibited the highest binding (8.14–8.56%) to the bacterial pellet followed by $^{99m}Tc(CO)_3$-**2** (7.51–7.92%) and $^{99m}Tc(CO)_3$-**3** (7.53–7.76%). The above ranges are for three different radioactive concentrations. No significant change in binding was observed after incubation of the radiopharmaceuticals with the bacteria that had been pre-exposed to a 50-fold excess of unlabeled ligands for 1 h, indicating non-specific binding. There was no significant change in binding with increase or decrease in the drug level in the radioactive dose. The viability of the cell suspension was not affected after 2 h of incubation with $^{99m}Tc(CO)_3$–thiosemicarbazones. The above experiments were repeated with $^{99m}TcO_4^-$ where three randomly selected bacterial samples were incubated with three aliquots of aqueous $^{99m}TcO_4^-$ (activity range 185–525 kBq), showing significantly lower binding (0.67–0.74%) to the above bacterial culture than that observed with $^{99m}Tc(CO)_3$–thiosemicarbazones. No change in the bacterial count was observed after 2 h of incubation. Also no evidence of an antibacterial effect of radioactivity within the stated range was found.

Biodistribution studies

The results of the biodistribution studies of the complexes in rats exposed to *S. aureus* infection and having sterile inflammation (turpentine) for different time periods are shown in

Table 3 Selected bond angles (°) of $Re(CO)_3$–thiosemicarbazones

Angle	*trans*-(*E*)-$ReBr(CO)_3$-**1a**	Angle	$[Re(CO)_3$-**1**$]_2$	Angle	*trans*-(*E*)-$ReBr(CO)_3$-**2a**	Angle	*cis*-(*Z*)-$ReBr(CO)_3$-**2b**	Angle	$[Re(CO)_3$-**2**$]_2$	Angle	$[Re(CO)_3$-**3**$]_2$
C1–Re1–C3	91.0(3)	C2–Re1–C1	90.0(3)	C1–Re1–C3	88.3(5)	C1–Re1–C2	88.7(7)	C2A–Re1A–C1A	88.2(6)	C2–Re1–C1	86.9(12)
C2–Re1–C1	86.0(3)	C3–Re1–C1	89.2(3)	C2–Re1–C1	86.5(6)	C3–Re1–C2	89.5(6)	C3A–Re1A–C2A	89.2(7)	C2–Re1–C3	90.3(14)
C2–Re1–C3	89.1(3)	C3–Re1–C2	89.6(3)	C2–Re1–C3	89.3(5)	C3–Re1–C1	90.3(6)	C3A–Re1A–C1A	88.5(6)	C1–Re1–C3	88.5(13)
C2–Re–Br1	93.7(2)	N1–Re1–S1	78.66(12)	C2–Re–Br1	176.9(4)	C2–Re1–Br3	89.9(4)	N1A–Re1A–S1A	78.0(2)	N3–Re1–S1	78.2(5)
C3–Re–Br1	89.0(2)	N1–Re1–S2	87.47(12)	C3–Re–Br1	89.1(4)	C1–Re1–Br3	93.5(4)	N1A–Re1A–S2A	87.9(3)	N3–Re1–S1^1	89.3(6)
C1–Re1–S1	95.15(19)	C1–Re1–S1	95.62(19)	C1–Re–S	95.2(4)	C1–Re1–S1	173.8(5)	C1A–Re1A–S1A	175.8(4)	C2–Re1–S1	94.3(9)
C2–Re1–S1	94.5(2)	C2–Re1–S1	174.11(19)	C2–Re–S	94.5(4)	C2–Re1–S1	97.3(4)	C2A–Re1A–S1A	95.1(4)	C1–Re1–S1	97.0(8)
C3–Re1–S1	173.1(2)	C3–Re1–S1	92.28(19)	C3–Re–S	175.0(3)	C3–Re1–S1	88.5(4)	C3A–Re1A–S1A	94.2(5)	C3–Re1–S1	173.0(10)
N1–Re1–S1	79.15(14)	C1–Re1–N1	173.0(2)	N1–Re–S	78.9(2)	N3–Re1–S1	79.6(3)	C2A–Re1A–N1A	172.5(4)	C1–Re1–N3	175.2(10)
C1–Re1–N1	96.9(2)	C2–Re1–N1	95.6(2)	C1–Re1–N1	172.6(4)	C1–Re1–N3	94.4(6)	C3A–Re1A–N1A	94.2(6)	C2–Re1–N3	92.8(10)
C2–Re1–N1	173.2(2)	C3–Re1–N1	94.9(2)	C2–Re1–N1	98.4(4)	C2–Re1–N3	175.7(5)	C1A–Re1A–N1A	98.6(5)	C3–Re1–N3	96.4(11)
C3–Re1–N1	96.9(9)	C1–Re1–S2	87.87(19)	C3–Re1–N1	97.3(4)	C3–Re1–N3	93.4(5)	C3A–Re1A–S2A	176.4(5)	C1–Re1–S1	97.0(8)
C1–Re1–Br1	179.7(2)	C2–Re1–S2	95.31(19)	C1–Re1–Br1	90.8(4)	C3–Re1–Br3	176.2(4)	C1A–Re1–S2A	94.1(4)	C1–Re1–S1^1	90.7(9)
N1–Re1–Br1	83.36(14)	S1–Re1–S2	83.08(5)	N1–Re1–Br1	84.39(18)	N3–Re1–Br3	87.1(3)	S1A–Re1A–S2A	83.32(9)	S1–Re1–S1^1	81.7(2)
C2–Re1–C1	86.0(3)	C2–Re1–C1	90.0(3)	C1–Re1–C3	88.3(5)	C1–Re1–C2	88.7(7)	C2A–Re1A–C1A	88.2(6)	C2–Re1–C1	86.9(12)

Table 4 Cyclic voltammetric parameters for the reduction of Re(I) thiosemicarbazone complexes measured in DMF at 100 mV s^{-1}

Compound	E_{pIIIc} (V)	E_{pIIIa} (V)	ΔE (V)	$E_{1/2}$ (V)	E_{pIVc} (V)
trans [$ReBr(CO)_3$-**2a**]	−0.83	−0.69	0.14	−0.76	−1.45
cis [$ReBr(CO)_3$-**2b**]	−0.80	−0.65	0.15	−0.73	−1.40

Table 6. Following an intravenous injection, the drugs were widely distributed in the animal body and excreted mainly through the hepatobiliary route. For all the ^{99m}Tc labeled thiosemicarbazones the uptake in the infected muscle was determined at 4, 8 and 24 h after injection. The percent injected dose per g of bacteria infected or of the inflamed right thigh muscle/control left thigh muscle was also determined in the above three post injection time periods. The uptake of the radiopharmaceuticals in the infected muscle was moderate at the initial time periods (4 and 8 h) and gradually became less up to 24 h. Infection *vs.* the normal tissue ratio was the highest for $^{99m}Tc(CO)_3$-**3** (4.62 : 1 at 4 h post injection). The uptake in the inflamed muscle was also low. The blood pool activity of the radiopharmaceuticals was considerably high and clearance from the blood was very slow. This resulted in comparatively higher uptake levels in the liver, lung and spleen. The compounds being lipophilic in nature are excreted mainly through the hepatobiliary route. Localization of the radioactivity in the liver and intestine was considerably high. Both $^{99m}Tc(CO)_3$-**1** and $^{99m}Tc(CO)_3$-**2** initially exhibited high accumulation in the liver which gradually cleared out from the organ. But $^{99m}Tc(CO)_3$-**3** being most lipophilic exhibited very poor clearance and a substantial amount of activity was retained in the liver throughout the period of study. The accumulation of radioactivity in the kidney was considerably less (<1% ID per organ) resulting in poor renal excretion for all groups. Accumulation of radioactivity in the stomach for all the studied groups was significantly less, indicating the *in vivo* stability of the labeled complexes.

Scintigraphic imaging studies performed in the rat infection model revealed the potentiality of $^{99m}Tc(CO)_3$–thiosemicarbazones for the detection of bacterial infection. Retention of the radiopharmaceuticals at *S. aureus* infected rat thigh muscle at 4 and 8 h post injection time period is shown in Fig. 8. The results were in accordance with the biodistribution results in rats. The figures demonstrate the accumulation of higher activity in the infected region as compared to the non-infected tissues. They also reveal substantial accumulation of the complexes in the liver and intestine suggesting that the major route of excretion was hepatobiliary.

Thiosemicarbazones have been a subject of interest to researchers of different disciplines due to their wide array of pharmacological properties. Because of their potential antibacterial and antiparasitic properties, studies of the co-ordination chemistry of their transition metal complexes have been the subject of interest in the biomedical field over the past few years. Surprisingly, little is known about the technetium complexes of thiosemicarbazones. Considering the importance of technetium in the radiopharmaceutical field, namely, in nuclear medicine, as well as the versatile application of organometallic complexes in biological sciences we have radiolabeled methyl, ethyl, and phenyl nitrofuryl thiosemicarbazones with the organometallic *fac*-$[^{99m}Tc(CO)_3(H_2O)_3]^+$ precursor and studied their antibacterial activities in *in vitro* and *in vivo* systems. Chelation chemistry and the steric profile are important considerations for the design of kinetically stable small molecule imaging agents. Therefore, detailed structural information was obtained by preparing the corresponding rhenium(I) complexes as rhenium serves as an effective non-radioactive chemical surrogate for technetium.

In vitro stability studies of $^{99m}Tc(CO)_3$-**1**, $^{99m}Tc(CO)_3$-**2** and $^{99m}Tc(CO)_3$-**3** in saline and serum revealed minimal decomposition of the label from the radiopharmaceuticals. Even after an incubation period of 24 h, there was only 7–9% decrease in the labeling efficiency, indicating the prolonged stability of the

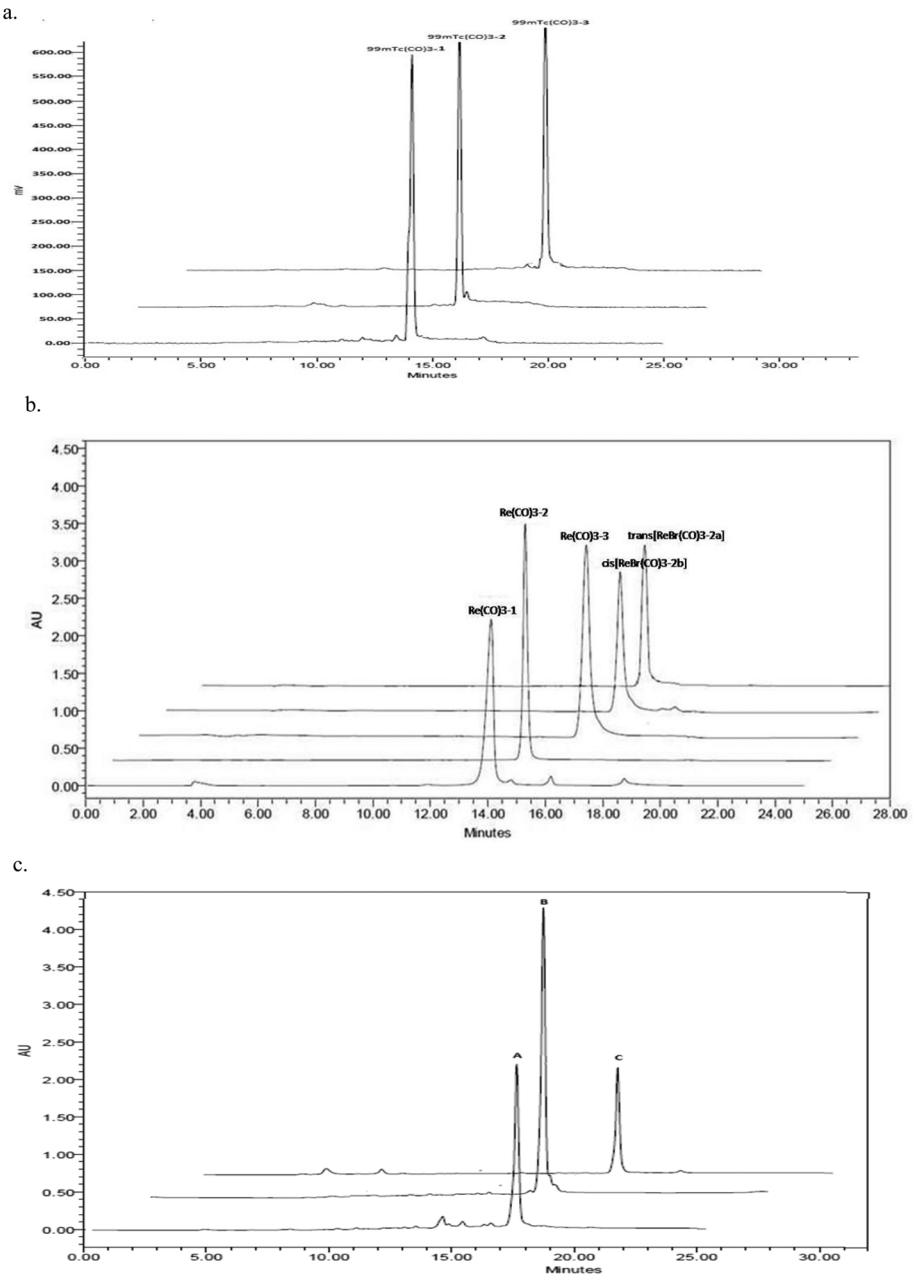

Fig. 7 (a) HPLC analysis profiles of $^{99m}Tc(CO)_3$-complexes of ligands **1**, **2**, and **3**. (b) HPLC analysis profiles of $Re(CO)_3$-complexes of ligands **1**, **2**, and **3**, as obtained from respective reaction mixtures and chromatograms of *trans*-[$ReBr(CO)_3$-**2a**], and *cis*-[$ReBr(CO)_3$-**2b**]. (c) HPLC chromatograms of dimeric $Re(CO)_3$ complexes of ligand **1** (A), ligand **2** (B), and ligand **3** (C).

^{99m}Tc labeled preparations and the suitability of the radiolabeled drugs for *in vivo* studies. The present study thus brings out the suitability of $^{99m}Tc(CO)_3$–thiosemicarbazones for the detection of focal infection in the rat thigh muscle. The observations extend the scope of transition metal chelates of thiosemicarbazones for infection imaging/scintigraphy. The *in vitro* and *in vivo* study results have shown satisfactory radiolabeling of the thiosemicarbazone ligands with the $^{99m}Tc(CO)_3(H_2O)_3$ precursor, which was sufficiently stable up to 24 h and was excreted mainly through the hepatobiliary routes. The radiopharmaceuticals accumulated at the *in vivo* sites of bacterial infection and exhibited an adequate target to non-target ratio. However, their *in vitro* binding to microorganisms was not very significant and this could not be blocked with an excess of unlabeled thiosemicarbazones.

The biodistribution studies gave evidence that the resulting complexes were stable *in vivo* during the study period and exhibited some accumulation in infection foci in the rat thigh model. These justify further studies with other thiosemicarbazone ligands, which are in progress.

Table 5 *In vitro* binding assay reported as % radiotracer bound with *S. aureus*: (i) at three different doses either in the presence or absence of excess unlabeled drug and (ii) ^{99m}Tc-pertechnetate

Compound	^{99m}Tc(CO)$_3$-**1**			^{99m}Tc(CO)$_3$-**2**			^{99m}Tc(CO)$_3$-**3**			^{99m}Tc-pertechnetate		
	183 kBq (40 μL)	320 kBq (80 μL)	523 kBq (120 μL)	165 kBq (40 μL)	335 kBq (80 μL)	530 kBq (120 μL)	180 kBq (40 μL)	355 kBq (80 μL)	550 kBq (120 μL)	185 kBq	370 kBq	525 kBq
Incubation without excess drug	8.14 ± 0.14	8.56 ± 0.15	8.34 ± 0.20	7.92 ± 0.13	7.51 ± 0.17	7.64 ± 0.22	7.76 ± 0.15	7.62 ± 0.24	7.53 ± 0.26	0.67 ± 0.07	0.74 ± 0.09	0.69 ± 0.02
Incubation with excess drug	8.23 ± 0.21	8.37 ± 0.14	8.46 ± 0.15	7.84 ± 0.11	7.56 ± 0.18	7.69 ± 0.20	7.67 ± 0.15	7.70 ± 0.03	7.39 ± 0.06			

Experimental

All chemicals and solvents were either of analytical or HPLC grade and used without further purification. 5-Nitrofurfural, various thiosemicarbazides, *p*-TsOH, and bromopentacarbonyl rhenium(I) [Re(CO)$_5$Br] were purchased from Sigma-Aldrich. The other chemicals and solvents were procured from Merck India. $^{99m}TcO_4^-$ was obtained by 2-butanone extraction from 5 N NaOH solutions of $^{99}MoO_4^-$ (purchased from BARC, Mumbai, India). IR spectra were recorded on a Jasco 410 FTIR spectrometer using KBr pellets. The ^{1}H NMR spectra were recorded using a Bruker 300 DPX spectrometer. Mass spectra were recorded using a Micromass Q-Tof (ESI-MS) spectrometer or a Jeol JMS700 (FAB-MS) spectrometer. RP-HPLC studies were performed using a Waters Associates HPLC system equipped with a Waters 515 pump, and a 2489 dual wavelength absorbance detector. Radioactivity in the RP-HPLC eluates was monitored by using a Berthold LB-500 HERM radio HPLC monitor procured from Berthold Technologies GmbH, Germany. Various γ-countings were performed using a well-type γ-counter from Electronic Corporation of India (model LV4755). Cyclic voltammetry of monomeric Re(CO)$_3$-complexes was carried out using a PAR model 237A potentiostat/galvanostat.

General

Synthesis of ligands 1 to 3. Ligands **1** to **3** were synthesized according to a previously published procedure.[12] Briefly an equimolar mixture of 5-nitrofurfural and thiosemicarbazide was stirred in dry toluene at room temperature under a nitrogen atmosphere in the presence of *p*-TsOH (catalytic amounts) to produce the desired thiosemicarbazones in ~75% yield (Scheme 1).

Data for nitrofuryl methyl thiosemicarbazone (1). IR data (KBr, cm^{-1}): ν 3275m, 3210m, 3098m (NH), 1561s (C═N). ^{1}H NMR [δ (ppm), CD$_3$OD]: 3.16 (s, 3H, CH$_3$), 7.11 (d, 1H, furan H), 7.55 (d, 1H, furan H), 7.87 (s, 1H, –N═CH–). MS (ESI): *m*/*z* 229.0 [40%, (M + H)$^+$], 251.0 [100%, (M + Na)$^+$]. Anal. Calcd for $C_7H_8N_4O_3S$: C, 36.8; H, 3.5; N, 24.5; S, 14.0. Found: C, 36.4; H, 3.6; N, 24.2; S, 13.8.

Data for nitrofuryl ethyl thiosemicarbazone (2). IR data (KBr, cm^{-1}): ν 3359m, 3104m, 2966m (NH), 1549s (C═N). ^{1}H NMR [δ (ppm), CD$_3$OD]: 1.26 (t, 3H, CH$_3$), 3.72 (q, 2H, CH$_2$), 7.12 (d, 1H, furan H), 7.55 (d, 1H, furan H), 7.87 (s, 1H, –N═CH–). MS (ESI): *m*/*z* 243.1 [20%, (M + H)$^+$], 265.1 [100%, (M + Na)$^+$]. Anal. Calcd for $C_8H_{10}N_4O_3S$: C, 39.7; H, 4.2; N, 23.1; S, 13.2. Found: C, 39.4; H, 4.6; N, 22.7; S, 12.8.

Data for nitrofuryl phenyl thiosemicarbazone (3). IR data (KBr, cm^{-1}): ν 3342m, 3110m, 2965m (NH), 1542s (C═N). ^{1}H NMR [δ (ppm), CD$_3$OD]: 7.21 (d, 1H, furan H), 7.26 (m, 1H, phenyl H), 7.39 (t, 2H, phenyl H), 7.58 (d, 1H, furan H), 7.62 (m, 2H, phenyl H), 7.96 (s, 1H, –N═CH–). MS (ESI): *m*/*z* 313.1 [100%, (M + Na)$^+$]. Anal. Calcd for $C_{12}H_{10}N_4O_3S$: C, 49.6; H, 3.5; N, 19.3; S, 11.0. Found: C, 49.4; H, 3.7; N, 19.1; S, 10.8.

^{99m}Tc-radiolabeling

Preparation of ^{99m}Tc(I)-synthon [^{99m}Tc(H$_2$O)$_3$(CO)$_3$]$^+$. The tricarbonyl precursor was prepared as per the method reported by us.[24] Briefly, an aqueous solution (2 mL) of NaBH$_4$ (11 mg), Na$_2$CO$_3$ (8 mg) and Na/K tartrate (30 mg) taken in a sealed glass vial was purged with CO gas (10–12 min). After the addition of an aqueous solution of $^{99m}TcO_4^-$ (1 mL, 200–250 MBq), the vial was heated at 75 °C for 20 min. After cooling the vial and re-equilibrating with atmospheric pressure, the pH of the reaction mixture was adjusted to 7 using a mixture of 0.5 M phosphate buffer (pH 7.5) : 1 M HCl (1 : 3). The synthon thus prepared was characterized by RP-HPLC.

Labeling of ligands (1 to 3) with the [^{99m}Tc(H$_2$O)$_3$(CO)$_3$]$^+$ precursor. Under optimized conditions, 0.8 mL of the freshly prepared [^{99m}Tc(H$_2$O)$_3$(CO)$_3$]$^+$ precursor (120–150 MBq) was added to the ligand solution (2–2.5 mg dissolved in 0.2 mL of the EtOH–H$_2$O mixture). The mixture was heated at 75 °C for 20 min and the pH was maintained between 7 and 7.5 (Scheme 1). The purities of ^{99m}Tc(CO)$_3$-complexes were ascertained by TLC and RP-HPLC.

General synthesis of the Re(CO)$_3$-complexes of ligands (1 to 3). To a solution of the ligand (0.25 mmol) in freshly distilled toluene (50 mL) was added an equimolar quantity of Re(CO)$_5$Br. The mixture was refluxed for 3 h, then concentrated *in vacuo* to *ca.* 15 mL and maintained at room temperature for several hours (Scheme 1). A reddish brown solid that precipitated was filtered off, recrystallised from acetone and dried in vacuum.

Table 6 Comparative results of biodistribution studies of $^{99m}Tc(CO)_3$–thiosemicarbazone in bacteria infected and inflamed Sprague–Dawley rats. Results are expressed in percent-injected dose per organ/tissue (each value is the mean ± SD of five rats per group)

Compounds	Time	Urine	Kidney	Liver	Intestine	Heart[a]	Blood[a]	Stomach[a]	Lung[a]	Spleen[a]	Muscle[a]	Infected muscle[a]	Ratio of infection/normal
$^{99m}Tc(CO)_3$-	4 h	4.97 ± 0.39	0.83 ± 0.09	16.39 ± 1.39	39.16 ± 2.68	0.14 ± 0.04	0.19 ± 0.03	0.64 ± 0.08	0.87 ± 0.17	0.33 ± 0.02	0.03 ± 0.00	0.13 ± 0.01	4.33 ± 0.17
1	8 h	16.67 ± 1.17	0.82 ± 0.20	7.73 ± 1.08	48.94 ± 0.85	0.14 ± 0.01	0.22 ± 0.02	0.82 ± 0.09	0.64 ± 0.11	0.30 ± 0.01	0.02 ± 0.00	0.10 ± 0.00	4.44 ± 0.48
	24 h		0.64 ± 0.11	4.49 ± 0.17	44.11 ± 1.36	0.09 ± 0.01	0.11 ± 0.03	0.41 ± 0.15	0.27 ± 0.07	0.53 ± 0.19	0.02 ± 0.00	0.08 ± 0.00	3.87 ± 0.45
$^{99m}Tc(CO)_3$-	4 h	7.41 ± 1.44	0.90 ± 0.11	18.25 ± 3.89	43.64 ± 3.13	0.17 ± 0.04	0.35 ± 0.08	0.27 ± 0.06	0.74 ± 0.14	0.40 ± 0.14	0.03 ± 0.00	0.16 ± 0.01	4.04 ± 0.28
2	8 h	9.41 ± 1.57	0.78 ± 0.32	4.52 ± 0.90	47.44 ± 3.27	0.16 ± 0.04	0.26 ± 0.08	0.33 ± 0.03	0.65 ± 0.26	0.34 ± 0.05	0.04 ± 0.01	0.17 ± 0.04	4.31 ± 0.36
	24 h		0.73 ± 0.06	3.14 ± 1.23	38.54 ± 1.04	0.08 ± 0.01	0.23 ± 0.00	0.36 ± 0.12	0.51 ± 0.09	0.75 ± 0.16	0.02 ± 0.00	0.09 ± 0.00	3.80 ± 0.26
$^{99m}Tc(CO)_3$-	4 h	4.36 ± 0.64	0.54 ± 0.11	3.63 ± 0.82	36.18 ± 8.04	0.14 ± 0.03	0.37 ± 0.05	0.21 ± 0.02	0.68 ± 0.06	0.62 ± 0.07	0.03 ± 0.00	0.13 ± 0.01	4.62 ± 0.35
3	8 h	6.46 ± 0.21	0.72 ± 0.21	21.59 ± 1.81	38.45 ± 0.82	0.17 ± 0.05	0.31 ± 0.07	0.42 ± 0.03	0.97 ± 0.12	1.01 ± 0.03	0.03 ± 0.00	0.14 ± 0.01	4.60 ± 0.20
	24 h		0.86 ± 0.16	24.14 ± 1.59	30.71 ± 0.92	0.19 ± 0.04	0.20 ± 0.03	0.29 ± 0.04	1.18 ± 0.11	1.71 ± 0.12	0.03 ± 0.00	0.12 ± 0.05	4.50 ± 0.12

	Time	Urine	Kidney	Liver	Intestine	Heart[a]	Blood[a]	Stomach[a]	Lung[a]	Spleen[a]	Muscle[a]	Inflammed muscle[a]	Ratio of inflammation/normal
$^{99m}Tc(CO)_3$-**1**	4 h	4.58 ± 1.20	1.92 ± 0.53	17.51 ± 0.82	35.39 ± 3.71	0.12 ± 0.02	0.24 ± 0.03	0.68 ± 0.19	0.77 ± 0.14	0.47 ± 0.09	0.03 ± 0.00	0.06 ± 0.00	2.02 ± 0.08
$^{99m}Tc(CO)_3$-**2**	4 h	5.62 ± 0.67	1.27 ± 0.32	19.64 ± 0.84	36.78 ± 4.51	0.16 ± 0.04	0.29 ± 0.07	0.54 ± 0.10	0.69 ± 0.08	0.37 ± 0.17	0.03 ± 0.00	0.07 ± 0.00	2.31 ± 0.12
$^{99m}Tc(CO)_3$-**3**	4 h	1.51 ± 0.50	1.69 ± 0.24	4.07 ± 5.87	26.05 ± 6.62	0.18 ± 0.01	0.44 ± 0.15	0.49 ± 0.07	0.73 ± 0.05	0.75 ± 0.14	0.03 ± 0.00	0.07 ± 0.00	2.26 ± 0.13

[a] Percent injected dose per g of tissue.

Data for $Re(CO)_3$-nitrofuryl methyl thiosemicarbazone [Re-(CO)$_3$-1]. Yield: 101 mg (81%). IR data (KBr, cm^{-1}): ν 3348 (NH), 2027, 1909 (CO_{fac}). ^1H NMR [δ (ppm), CD_3OD]: 2.85 (s, 6H, CH_3), 7.41 (m, 2H, furan H), 7.58 (m, 2H, furan H), 8.04 (s, 2H, –N═CH–). MS (ESI): *m*/*z* 498.9 [100%, $(M/2 + H)^+$], 470.9 [35%, $(M/2 - CO + H)^+$]. Anal. Calcd for $C_{20}H_{14}N_8O_{12}S_2Re_2$: C, 24.1; H, 1.6; N, 11.2; S, 6.4. Found: C, 23.8; H, 1.8; N, 10.9; S, 6.3.

The reddish brown solid was dissolved in acetone and few drops of ethanol (C_2H_5OH) were added to obtain dark brown single crystals of $[Re(CO)_3\text{-}\mathbf{1}]_2{\cdot}C_3H_6O$ suitable for X-ray diffraction.

Data for $Re(CO)_3$-nitrofuryl ethyl thiosemicarbazone [Re-(CO)$_3$-2]. Yield: 121 mg (79%). IR data (KBr, cm^{-1}): ν 3400 (NH), 2022, 1909 (CO_{fac}). ^1H NMR [δ (ppm), acetone-d_6]: 1.31 (t, 6H, CH_3), 3.63 (br s, 4H, CH_2), 7.59–7.64 (m, 4H, furan-H), 8.50 (br s, 2H, –N═CH–). MS (ESI): *m*/*z* 512.9 [100%, $(M/2 + H)^+$], 484.9 [20%, $(M/2 - CO + H)^+$]. Anal. Calcd for $C_{22}H_{18}N_8O_{12}S_2Re_2$: C, 22.3; H, 1.7; N, 9.4; S, 5.4. Found: C, 22.0; H, 1.9; N, 9.2; S, 5.3.

The reddish brown solid precipitated upon the concentration of the reaction mixture was redissolved in acetone and few drops of methanol were added when dark brown single crystals of the dimer $[Re(CO)_3\text{-}\mathbf{2}]_2{\cdot}C_3H_6O{\cdot}CH_3OH$ suitable for X-ray studies were furnished.

In a separate experiment, slow evaporation of the reaction mixture (toluene) of the complex produced two different types of single crystals (isomers **2a** and **2b**) of $ReBr(CO)_3$–$\mathbf{2}{\cdot}C_7H_8$ suitable for X-ray diffraction.

Data for *trans*-[ReBr(CO)$_3$-2a]. IR data (KBr, cm^{-1}): ν 3350 (NH), 2029, 1926, 1902 (CO_{fac}). ^1H NMR [δ (ppm), acetone-d_6]: 1.32 (t, 3H, CH_3), 3.68 (m, 2H, CH_2), 7.78–7.83 (m, 2H, furan-H), 8.67 (m, 1H, –N═CH–); additional peaks around 7.22 and 2.32 (ppm) are attributed to toluene used as the solvent for crystallization. MS (ESI): *m*/*z* 513.1 [45%, $(M - Br)^+$], 485.1 [100%, $(M - Br - CO)^+$].

Data for *cis*-[ReBr(CO)$_3$-2b]. IR data (KBr, cm^{-1}): ν 3350 (NH); 2028, 1926, 1900 (CO_{fac}). ^1H NMR [δ (ppm), acetone-d_6]: 1.32 (t, 3H, CH_3), 3.69 (m, 2H, CH_2), 7.80–7.83 (m, 2H, furan-H), 8.53 (m, 1H, –N═CH–); additional peaks around 7.22 and 2.32 (ppm) are attributed to toluene used as the solvent for crystallization. MS (ESI): *m*/*z* 512.9 [75%, $(M - Br)^+$], 484.9 [100%, $(M - Br - CO)^+$].

Data for $Re(CO)_3$-nitrofuryl phenyl thiosemicarbazone [Re-(CO)$_3$-3]. Yield: 124 mg (85%). IR data (KBr, cm^{-1}): ν 3252 (NH), 2029, 1914 (CO_{fac}). ^1H NMR [δ (ppm), acetone-d_6]: 7.40 (m, 2H, furan-H), 7.55 (m, 8H, phenyl-H), 7.81 (m, 4H, phenyl-2H, furan-2H), 8.62, 8.81 (s, 2H, –N═CH–). MS (ESI): *m*/*z* 1143.0 [85%, $(M + Na)^+$], 583.0 [100%, $(M/2 + Na)^+$], 561.0 [30%, $(M/2 + H)^+$], 533.0 [30%, $(M/2 - CO + H)^+$]. Anal. Calcd for $C_{30}H_{20}N_8O_{12}S_2Re_2$: C, 32.1; H, 1.8; N, 10; S, 5.7. Found: C, 32.0; H, 2.1; N, 9.8; S, 5.6.

Red colored single crystals of $[Re(CO)_3\text{-}\mathbf{3}]_2{\cdot}2CH_3OH$ suitable for X-ray diffraction were obtained by slow evaporation of a methanolic solution of the reddish brown solid isolated from the reaction mixture.

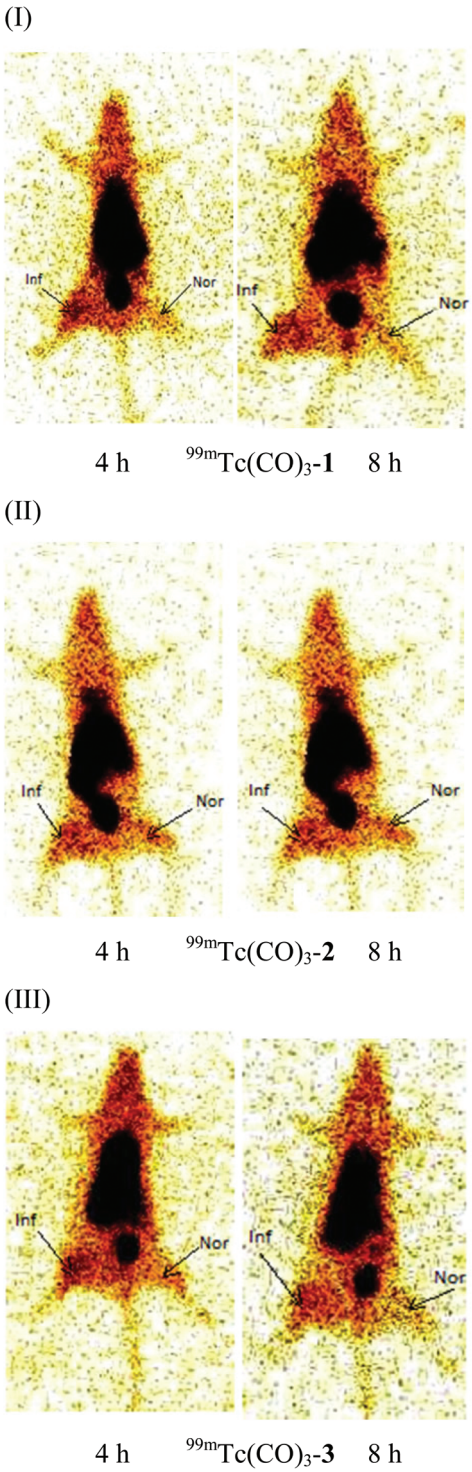

Fig. 8 Scintigraphic images of ^{99m}Tc(CO)$_3$–thiosemicarbazone in *S. aureus* infected rats at 4 h and 8 h post-injection (i.v.): (I) ^{99m}Tc(CO)$_3$-**1**, (II) ^{99m}Tc(CO)$_3$-**2**, (III) ^{99m}Tc(CO)$_3$-**3**.

Crystal structure analysis

X-ray data collection, structure determination, and refinement. Crystallographic data were collected on a Kappa APEX II Bruker SMART CCD area-detector system (Bruker Advanced X-Ray Solutions, USA) at 296 K. Suitable crystals were mounted on a capillary using a Crystal Logic Synchrotron Goniometer flat diffractometer that used graphite monochromated Mo Kα radiation. The structures were solved by direct methods using the program SHELXTL and refined by the full-matrix least squares techniques on F^2 using SHELXL-2013. The crystallographic data and structure refinement parameters are shown in Table 2, while the selected bond angles and distances are shown in Table 3 and below the respective figures respectively.

Quality control techniques

Thin layer chromatography. The radiochemical purities of ^{99m}Tc(CO)$_3$-complexes of ligands **1–3** were determined by instant thin layer chromatography (ITLC) on silica gel 60 F254 strips (1 × 8 cm, Merck KGaA, Darmstadt, Germany) spotted with radioactive complexes and developed with methyl ethyl ketone (MEK, system A) and brine (system B). The R_f values of the ^{99m}Tc-complexes, $^{99m}TcO_4^-$, and $[^{99m}Tc(H_2O)_3(CO)_3]^+$ are respectively 0, 1 and 0 in system A and 1, 1 and 0 in system B. Quantitative analysis was performed by cutting the strips into five pieces and counting them separately in a gamma counter (ECIL, India).

Reverse-phase high-performance liquid chromatography (RP-HPLC) analysis

The radiolabeling yields as well as characterization of the $[^{99m}Tc(H_2O)_3(CO)_3]^+$ precursor, and ^{99m}Tc(CO)$_3$ and Re(CO)$_3$-complexes of ligands **1** to **3** were obtained by RP-HPLC analysis using a Waters (USA) XTerra RP18 column (4.6 mm × 250 mm, particle size, 5 μm) eluting with a gradient mixture of 0.1% TFA in water (eluent A) and acetonitrile (eluent B). A linear gradient was run at a flow rate of 1 mL min^{-1} for 0–25 min (0–15 min: 90% A/10% B to 10% A/90% B and changing to initial conditions between 15 and 25 min).

In vitro stability

The *in vitro* stability of the ^{99m}Tc(CO)$_3$–thiosemicarbazone complexes (**1–3**) was checked separately in normal saline and freshly collected rat serum at different time intervals. A 0.1 mL aliquot of each of the radiolabeled complexes was added separately to 0.9 mL of (a) saline and (b) serum, and incubated at 37 °C for 24 h. Samples were withdrawn from the mixture at 0, 0.5, 2, 4, and 24 h and analyzed by ITLC (silica gel plates/methyl ethyl ketone developing solvent). The stability of the radiolabeled complexes was also ascertained by His challenge experiment. 0.1 mL aliquots of each of the ^{99m}Tc(CO)$_3$-complexes were added to 0.9 mL of 10^{-3} M histidine solution in phosphate buffer (pH 7.4). The mixtures were incubated for 24 h at 37 °C and analyzed by ITLC (as above) at 1, 4 and 8 h. All the results are expressed as mean ± SD of three experiments.

Octanol water partition coefficient measurement

The partition coefficient values (log $P_{o/w}$) of the ^{99m}Tc(CO)$_3$–thiosemicarbazone complexes (**1–3**) were determined by adding 0.1 mL of each of the radiolabeled complexes to a cen-

trifuge tube containing 1 mL 1-octanol and 1 mL phosphate buffer (0.025 M, pH 7.4). Each mixture was vortexed at room temperature for 2 min and then centrifuged at 3350*g* for 5 min. From each phase equal aliquots (0.1 mL) of the organic and aqueous layers were withdrawn and counted separately in an ECIL gamma counter. Each measurement was repeated three times. Care was taken to avoid intermixing between the phases. The partition coefficient (*P*) was calculated using the following equation: *P* = cpm in octanol − cpm in background/cpm in buffer − cpm in background and expressed as log $P_{o/w}$.

Cyclic voltammetry

Cyclic voltammetry of the monomeric $Re(CO)_3$ complex of nitrofuryl ethyl thiosemicarbazone was carried out in DMF (*ca.* 10×10^{-3} mol L^{-1}), under a nitrogen atmosphere at room temperature with TBAP (*ca.* 0.1 mol L^{-1}) as the supporting electrolyte. A Pt electrode (2 mm diameter) was used as a working electrode and a Pt wire as a counter electrode. The measurements were made against an Ag/AgCl reference electrode with scan rates varying from 50 mV s^{-1} to 1000 mV s^{-1}.

In vitro bacterial binding study

Binding of $^{99m}Tc(CO)_3$–thiosemicarbazone complexes of ligands **1–3** to a freshly prepared harvested culture of *S. aureus* was assessed at 37 °C as per the reported method with some modifications.[29] Briefly, to each of three sterile Eppendorf vials containing 1 mL of sterile PBS (0.1 mol L^{-1}, pH 7.4) and 0.1 mL of the freshly prepared *S. aureus* culture (1×10^8 cfu mL^{-1}), one of the three different aliquots (40, 80 and 120 μL) of $^{99m}Tc(CO)_3$–thiosemicarbazone complex solutions was added. The mixtures were incubated for 1 h at 37 °C and then centrifuged at 2000*g* for 5 min. The supernatants from each of the three vials were transferred to three different test tubes. The bacterial pellet was gently resuspended in sterile cold PBS (1 mL), and recentrifuged as above; the supernatant was transferred to the respective previous vials containing the first supernatant. The supernatants and pellets of each vial were counted (ECIL γ-counter) separately against suitably diluted aliquots of added radioactivity (to each vial) as the standard. For each concentration of each of the radiolabeled thiosemicarbazones, the experiments were repeated four times and the results are expressed as the mean ± S.D. The above procedure was also repeated with $^{99m}TcO_4^-$ (185, 370 and 525 kBq) in separate experiments. The experiments for each concentration of each of the radiolabeled complexes were also repeated simultaneously in the presence of 50-fold excess of unlabeled ligands to determine the specificity of $^{99m}Tc(CO)_3$-labeled thiosemicarbazone binding to bacteria. The bacterial culture was preincubated for 1 h with excess unlabeled thiosemicarbazones and all other processes were similar as before.

Induction of infectious foci and non-infected inflammation in rats

A freshly prepared harvested culture of *S. aureus* (1×10^8 cfu mL^{-1}) in 0.1 M PBS (pH 7.4) was used to produce a focal infection and 0.2 mL of the above bacterial suspension was injected into the right thigh muscle of each rat (body weight of 250 g). After 24 h the infection was apparent from swelling and reddening of the inoculated muscle. Similarly sterile inflammation was induced by injecting 0.1 mL of turpentine oil into the right thigh muscle of each rat belonging to a separate group. Swelling appeared 24 h later. All the animal experiments were approved by the Social Justice and Empowerment Committee for the purpose of control and supervision of experiments on animals (CPCSEA), Government of India, New Delhi.

Animal biodistribution studies

$^{99m}Tc(CO)_3$–thiosemicarbazone complexes (5–10 MBq per kg body wt) were injected into the anaesthetized (ketamine 30–50 mg kg^{-1} IM) rats through a precannulated femoral vein. The animals were sacrificed at 4, 8, or 24 h post injection. Muscles from both infected and normal thighs and other organs of interest were excised, rinsed with normal saline and blotted dry to remove any residual blood. Blood samples and urine were obtained by puncture of the heart and urinary bladder respectively. Radioactivity of all samples was measured using a well-type NaI(Tl) scintillation counter (ECIL, India) against suitably diluted aliquots of the injected solution as standards. The results are expressed either as percentage injected dose per gram of tissue or percentage injected dose per organ. Similar experiments were performed in the rat model of turpentine induced sterile abscess. Abscess to muscle activity ratios were calculated in both the infection and sterile inflammation models.

Conclusion

In summary three nitrofuryl thiosemicarbazone ligands were successfully radiolabeled with the *fac*-$[^{99m}Tc(H_2O)_3(CO)_3]^+$ core. The *in vitro* results have shown satisfactory radiolabeling of the ligands with tricarbonyl technetium. The *in vivo* behavior of the complexes was evaluated by biodistribution studies in the infected rat model. The reactions of $ReBr(CO)_5$ with different nitrofuryl thiosemicarbazone ligands yielded the corresponding $Re(CO)_3$–thiosemicarbazone complexes, which were characterized by X-ray crystallography. The structure elucidation helped us in understanding the coordination chemistry of thiosemicarbazone ligands with the technetium metal which will be useful in designing new target specific ^{99m}Tc and $^{186/188}Re$–thiosemicarbazone radiopharmaceuticals based on the tricarbonyl concept. Electrochemical behaviors of monomeric complexes mainly focus on the reduction of the nitro group, which is a prerequisite for antibacterial effects. If suitably developed, these compounds can also be used for hypoxia imaging.

Statistical analysis

All mean values of animal experiments are expressed as % ID per g of tissues or organs ± SD. The *p* values of the experi-

mental results were calculated and found to be <0.05 (statistically significant).

Conflict of interest

The authors declare no competing financial interest.

Acknowledgements

This work was funded by the Department of Atomic Energy, Mumbai (India) and by the Council of Scientific and Industrial Research (India), we thank both organisations for financial support. We thank Dr Basudeb Achari, Emeritus Scientist for his valuable suggestions during the preparation of the manuscript.

References

1 C. María, A. Rodríguez, C. Estefania, S. López, J. Sanmartín, P. Pelagatti and F. Zani, *J. Inorg. Biochem.*, 2005, **99**, 2231–2239.
2 M. Joseph, V. Suni, M. R. P. Kurup, M. Nethaji, A. Kishore and S. Bhat, *Polyhedron*, 2004, **23**, 69–3080.
3 L. Otero, M. Vieites, L. Boiani, A. Denicola, C. Rigol, L. Opazo, C. Olea-Azar, J. D. Maya, A. Morello, R. L. Krauth-Siegel, O. E. Piro, E. Castellano, M. González, D. Gambino and H. Cerecetto, *J. Med. Chem.*, 2006, **49**, 3322–3331.
4 S. N. Pandeya, D. Sriram, G. Nath and E. Declercq, *Eur. J. Pharm. Sci.*, 1999, **9**, 25–31.
5 E. Pahontu, V. Fala, A. Gulea, D. Poirier, V. Tapcov and T. Rosu, *Molecules*, 2013, **18**, 8812–8836.
6 M. R. Taylor, E. J. Gabe, J. P. Glusker, J. A. Minkin and A. L. Patterson, *J. Am. Chem. Soc.*, 1966, **88**, 1845–1846.
7 M. X. Li, C. L. Chen, D. Zhang, J. Y. Niu and B. S. Ji, *Eur. J. Med. Chem.*, 2010, **45**, 3169–7317.
8 B. Prathima, Y. S. Rao, G. N. Ramesh, M. Jagadeesh, Y. P. Reddy, P. V. Chalapathi and A. V. Reddy, *Spectrochim. Acta, Part A*, 2011, **79**, 39–44.
9 T. D. Thangadurai and K. Natarajan, *Transition Met. Chem.*, 2001, **26**, 717–722.
10 H. Beraldo and D. Gambinob, *Mini-Rev. Med. Chem.*, 2004, **4**, 31–39.
11 J. S. Casas, M. S. G. Tasende and J. Sordo, *Coord. Chem. Rev.*, 2000, **209**, 197–261.
12 G. Aguirre, L. Boiani, H. Cerecetto, M. Fernandez, M. Gonzalez, A. Denicola, L. Otero, D. Gambino, C. Rigol, C. Olea-Azar and M. Faundez, *Bioorg. Med. Chem.*, 2004, **12**, 4885–4893.
13 S. Sharma, F. Athar, M. R. Maurya, F. Naqvi and A. Azam, *Eur. J. Med. Chem.*, 2005, **40**, 557–562.
14 M. M. B. Pessoa, G. F. S. Andrade, M. R. Santos and M. L. A. Temperini, *J. Electroanal. Chem.*, 2003, **545**, 117–122.
15 S. N. Moreno, R. P. Mason and R. Docampo, *J. Biol. Chem.*, 1984, **259**, 6298–6305.
16 L. Otero, J. D. Maya, A. Morello, C. Rigol, G. Barriga, J. Rodriguez, C. Folch, E. Norambuena, M. Gonzalez, C. OleaAzar, H. Cerecetto and D. Gambino, *Med. Chem.*, 2008, **4**, 11–17.
17 R. E. Brown, F. A. Stancato and A. D. Wolfe, *Antimicrob. Agents Chemother.*, 1981, **19**, 234–237.
18 C. Bot, B. Hall and G. Alvarez, *Antimicrob. Agents Chemother.*, 2013, **57**, 1638–1647.
19 J. Turrens, *Mol. Aspects Med.*, 2004, **25**, 211–220.
20 E. M. Jouad, G. Larcher, M. Allain, A. Riou, G. M. Bouet, M. A. Khan and X. D. Thanh, *J. Inorg. Biochem.*, 2001, **86**, 565–571.
21 J. Taylor, D. Eshima, A. R. Fritzberg, P. E. Christian and S. Kasina, *J. Nucl. Med.*, 1986, **27**, 795–803.
22 R. D. Neirinckx, L. R. Canning, I. M. Piper, D. P. Nowotnik, R. D. Pickett, R. A. Holmes, W. A. Volkert, A. M. Forster, P. S. Weisner, J. A. Marriott and S. B. Chaplin, *J. Nucl. Med.*, 1987, **28**, 191–202.
23 R. Alberto, R. Schibli, A. Egli, P. A. Schubiger, U. Abram and T. A. Kaden, *J. Am. Chem. Soc.*, 1998, **120**, 7987–7988.
24 K. K. Halder, D. K. Nayak, R. Baishya, B. R. Sarkar, S. Sinha, S. Ganguly and M. C. Debnath, *Metallomics*, 2011, **3**, 1041–1048.
25 A. Montenegro, R. Carballo and E. M. Vazquez, *Polyhedron*, 2008, **27**, 2867–2876.
26 R. Carballo, J. Casas, E. Martínez, G. Pereiras-Gabian, A. Sanchez, J. Sordo, E. M. Vazquez-Lopez, J. C. Garcia-Monteagudo and U. J. Abram, *Organomet. Chem.*, 2002, **656**, 1–10.
27 C. Olea-Azar, C. Rigol, F. Mendizabal, A. Morello, J. D. Maya, C. Moncada, E. Cabrera, R. Dimaio, M. González and H. Cerecetto, *Free Radical Res.*, 2003, **37**, 993–1001.
28 C. Rigol, C. Olea-Azar, F. Mendizábal, L. Otero, D. Gambino, M. González and H. Cerecetto, *Spectrochim. Acta, Part A*, 2005, **61**, 2933–2938.
29 D. K. Nayak, R. Baishya, K. K. Halder, T. Sen, B. R. Sarkar, S. Ganguly, M. K. Das and M. C. Debnath, *Metallomics*, 2012, **4**, 1197–1208.